Originally published in *Proceedings of the Fifth International Workshop on Compressible Turbulent Mixing*, ed. R. Young, J. Glimm & B. Boston.
ISBN 9810229100, World Scientific (1996).

Two–Phase Flow Model for Rayleigh–Taylor and Richtmyer–Meshkov Mixing*

U. Alon[1,2] and D. Shvarts[1,3]

[1] Physics Department
Nuclear Research Center - Negev
P.O.B. 9001
Beer-Sheva, Israel

[2] Physics of Complex Systems
The Weizmann Institute of Science
Rehovot, 76100, Israel

[3] Laboratory of Laser Energetics
University of Rochester
250 East River Rd.
Rochester NY 14623

Abstract. A new realization of the two-phase flow approach is presented and applied for the Rayleigh-Taylor (RT) and Richtmyer-Meshkov (RM) instabilities. The mixing zone fronts and interior are treated separately, yielding a physically motivated model that is easier to implement numerically than standard two-phase flow treatments. In the model, the evolution of the mixing zone boundaries is given by point equations, based on the physics of large-scale structure at the fronts. The inner zone mixing is governed by a diffusive scheme that simplifies standard two-phase flow equations. The mixing-model parameters are determined by comparison to theoretical models. The linear stage and late-time growth scaling laws, for both RT and RM cases, as well as the mixing profiles, are obtained in good agreement with full-scale numerical simulations.

1 Introduction

The Rayleigh-Taylor (RT) [1] and Richtmyer-Meshkov (RM) [2] instabilities play a crucial role in ICF compression [3]. This process involves multi-mode perturbations growing in regimes of time dependent acceleration, compressibility, thermal conduction and multiple shocks in a complex geometry. The relevant perturbation modes may span several decades in wavelength [4]. It is thus impractical in many cases to perform

*Acknowledgment: UA thanks the Laboratory of Laser Energetics at the University of Rochester for their hospitality and partial support. It is a pleasure to thank C.P. Verdon, R.L. McCrory, R. Epstein, E.W. Burke, C. Cranfill, F. Harlow, D.H. Sharp and S.A. Orszag for stimulating discussions.

detailed direct numerical simulations of the instability growth. Existing theoretical treatments are limited to idealized situations [5, 6, 7, 8, 9, 10]. Simple mixing models are therefore needed to assess the effects of mixing in realistic situations.

A commonly proposed class of models are those based on turbulent transport [11, 12, 13]. An important feature of turbulence models is that both the inner zone structure and the evolution of the mixing zone boundaries are determined by the turbulent diffusion process. Turbulent transport models contain many empirical parameters, associated with the various closure approximations. Even the simplest turbulence models contain on the order of ten such parameters [11, 12, 13]. These parameters are typically calibrated based on developed turbulence experiments and models, as well as mixing experiments. However, the basic assumption made in such models, that the coarse-grained mixing zone evolution is primarily due to the small scale turbulent motion, seems to contradict numerical and theoretical evidence that suggest that the mixing front evolution is dominated by large structures [9, 10, 16, 17, 18]. This is reflected in the fact that in many studies, it has been found that it is difficult to obtain a set of model parameters that simultaneously reproduce numerical and experimental results for both RT and RM problems [12, 13, 16], and different parameter sets are needed to describe different experiments.

The large-structure nature of the flow is more naturally included in the two-phase flow (2PF) approach, which considers the flow as divided into regions rich with light fluid, that are correlated with an upwards velocity, and regions rich with heavy fluid that are correlated with a velocity in the opposite direction. The main large-scale features of the flow are captured by considering two phases, which obey conservation laws and interact with each other. The variables associated with these phases are the phase volume fraction f_i, the density ρ_i and the phase velocity u_i, as well as the phase internal energies and equations of state. In 2PF treatments [17, 19, 20, 21, 22, 14, 25, 27], the Euler equations, which are valid for the mean flow, are separated into two components, one for each phase. Each phase obeys separate mass and momentum equations, the latter with phenomenological drag and pressure partition terms.

This implementation of the 2PF approach suffers from several drawbacks. First, it is significantly more difficult to implement numerically [26] than diffusive-type mixing models. Second, in order to calibrate the model, it is necessary to solve the partial differential equations over the entire mixing zone. Since the front evolution and the inner-zone structure are linked in a complicated manner, it is not easy to point out the role of different parameters in controlling the front evolution.

Here we implement the 2PF approach in a new way which helps overcome these drawbacks. In the new model, the evolution of the fronts and the evolution of the inner-zone mixing are described by separate equations. These are cast in a form that is simple to handle numerically. In Sec 2 we describe ODE's for the bubble and spike fronts that mark the boundaries of the mixed region. These equations are obtained

by interpreting the 2PF equations at the fronts in terms of large-structure buoyancy and drag physics. In this way, the functional form and coefficients of these terms are determined by comparison to potential-flow [5, 33] and bubble-merger [6, 7, 9, 10] theories, that have yielded scaling-laws for the RT and RM instabilities. This allows both the bubble and spike, RT and RM, linear stage and late-time multimode scaling laws to be captured with a single set of parameters. In Sec 3, we outline a treatment of the inner-zone mixing, between the two fronts. A summary and discussion of the model results is given in Sec. 4. A detailed description of the model and further comparison with simulations will be presented in a forthcoming publication.

2 Point equations for the bubble and spike fronts

We consider the mixing of two fluids of densities ρ_i, where $i = 1$ denotes the lighter fluid and $i = 2$ the heavier fluid, under an acceleration $g(t)$. The Atwood ratio is $A = (\rho_1 - \rho_2)/(\rho_1 + \rho_2)$. ODE's for the location of the bubble and spike fronts are obtained based on the physics of the large structures that dominate these fronts. Based on the balance of buoyancy and kinematic drag on large fluid structures, [10, 31, 32], we employ the equation

$$dU_i/dt = C_{B,i}(A)g(t) - C_{D,i}(A)U_i|U_i|/L_i \tag{1}$$

where $U_i = dH_i/dt$ is the velocity of the front of fluid i, $C_{B,i}$ and $C_{D,i}$ are dimension-less constants that depend on the Atwood number and L_i is proportional to the dominant structure size. Note that this equation is valid also for $g < 0$, describing stable waves on the interface.

We first consider the bubble front. To obtain the coefficients for this case, we note that Eq. 1 is equivalent to Layzer's $A = 1$ single mode potential flow model [5] when using

$$C_{B,i} = A(1 - E)/(2 + E) \tag{2}$$

$$C_{D,i} = 6\pi/(2 + E) \tag{3}$$

where $E = exp(-6\pi H_1/L_1)$. In the linear stage, when $L_1(t) \approx L_1(t = 0) = \lambda_0$, where $\lambda_0 = 2\pi/k$ with k the mean initial perturbation wavenumber, we obtain both the RT and RM linear growth equations. At times somewhat after the perturbation reaches the nonlinear stage, the multi-mode fronts have been found to reach a scale-invariant regime [8, 9, 10] where the dominant mode's wavelength is proportional to the front penetration [10]. This suggests the following equation for the length scale (see also Ref [27])

$$dL_1/dt = \beta_1 U_1 \qquad L_1(t = 0) = \lambda_0 \tag{4}$$

where β_1 is a parameter that represents the effects of bubble competition in the multimode case. To find β_1 we use the RT scaling laws [1, 6, 7, 10, 33], and, as shown

below, get a satisfactory model for both RT and RM cases. In the RT case, $g(t) = g$, and using $H_1 = \alpha_B(A)gt^2$ we obtain from Eq 1 a relation between β_1 and α_B:

$$\alpha_B = C_{B,1}/(2 + 4C_{D,1}/\beta_1) \tag{5}$$

Layzer's model values for $C_{B,1}$ and $C_{D,1}$, Eqs. 2 and 3, approach $C_{B,1} = A/2$ and $C_{D,1} = 3\pi$ at late times. This suggests the value

$$\beta_1 \approx 2\pi \tag{6}$$

in order to get $\alpha_B \approx A/16 = 0.0625A$ in good agreement with experiment [18] simulations [6, 17, 20] and theory [7, 10]. We now use the same values of the parameters for the later-stage RM case, solving Eq 1 using an initial velocity $U_1(t = 0) = u_0$ and $g(t) = 0$. This yields as late times

$$H_1 \sim (u_0 t/\lambda_0)^{\theta_B} \qquad \theta_B = 1/(1 + C_{D,1}/\beta_1) = 0.4 \tag{7}$$

in good agreement with recent results [9, 10] coefficient values for both RT and RM suggests that the nonlinear evolution of both instabilities relies on similar large-structure physics. Note that the late-time RM front penetration, Eq. (7), depends at all times on u_0 and λ_0, the mean initial perturbation velocity and wavelength [9, 10, 27]. This is in contrast with the RT case, in which memory of the initial perturbations is lost.

Similar considerations are made for the spike front, with the same form for the front equation, Eq 1. In order to obtain the same linear growth rate for the bubbles and spikes, the value of the buoyancy coefficient is the same as in the bubble case (Eq. 5), $C_{B,2} = C_{B,1}$. A separate length-scale, L_2, is used to describe the spikes (L_1 and L_2 can be viewed as the values at the two fronts of a space dependent length-scale [25]):

$$dL_2/dt = \beta_2 U_2 \tag{8}$$

with $\beta_2 = \beta_1 = 2\pi$.

The spike drag coefficient is determined from the RT scaling laws

$$C_{D,2} = \pi(4/F(A) - 1) \tag{9}$$

where $F(A) = \alpha_S/\alpha_B$ is the ratio of spike and bubble front penetrations. We use a simple form for $F(A)$ based on numerical [17], experimental [18] and theoretical [10, 20] studies of α_S/α_B, where $F(A) \sim 1 + A$ at low A, and $F(A = 1) = 4$ (so that the spike drag vanishes at $A = 1$). Applying this to the RM case, yields $H_2 \sim (u_0 t/\lambda_0)^{\theta_S(A)}$. This implies a relation between $\alpha_S(A)$ and $\theta_S(A)$, which yields values for $\theta_S(A)$ in good agreement with theory and simulations [10, 28], where the exponent was found to rise with A, from $\theta_S(A) = 0.4$ at low A to $\theta_S(A = 1) = 1$. We note that the point equations may be easily applied to the case of time-dependent driving acceleration $g(t)$, yielding results in agreement with recent theoretical treatment of this case described elsewhere in this volume.

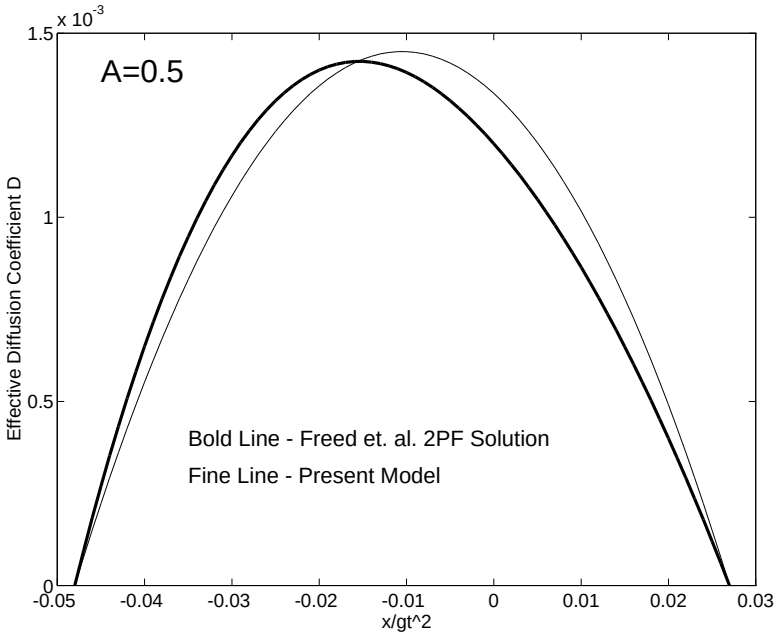

Figure 1: Diffusion coefficient from the self-similar 2PF solution of Ref. [20] (heavy line) and present model (light line). The self-similar mixing zone boundaries in the 2PF model are slightly different than the present point equations, especially in the spike front at high density ratios. Therefore, we use the 2PF solution values for the scaled front penetrations in the comparison. The Atwood number is A=0.5.

3 Mixing zone structure

We now consider the mixing zone inner structure. We work in a Lagrangian frame (which, in the presence of mixing, is defined so that Lagrangian cells contain a constant mass [12]), and incorporate the mixing model into a 1D hydrodynamic code in which the mean fluid velocity and internal energy are tracked. Consider for simplicity the case of two incompressible fluids. The mixing zone boundaries are tracked, by solving the front equations [Eq. 1]. The fluid volume fractions f_i are advected in a Lagrangian formulation according to [17] $\partial f_i/\partial t = \nabla \cdot (f_i u_i)$, which may be formally written as a diffusion equation:

$$\partial f_i/\partial t = \nabla \cdot (D \nabla f_i) \tag{10}$$

We obtain the effective diffusion coefficient, defined by $D = u_i f_i / \nabla f_i$ by comparison to an analytic solution of a 2PF model: in the incompressible RT case, an analytic solution

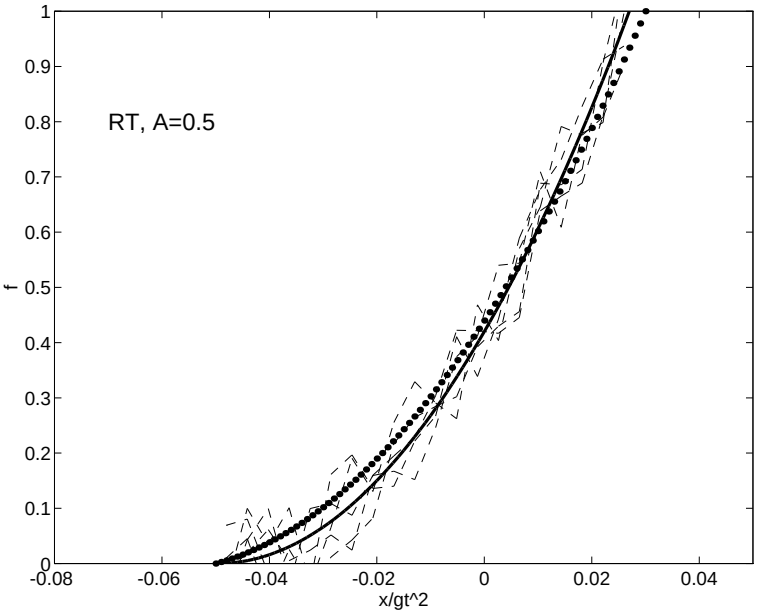

Figure 2: Heavy fluid volume fraction as a function of the scale invariant coordinate $s = x/gt^2$, in an incompressible RT case. Dashed lines are simulation results, full line is the Freed et. al. 2PF self-similar result, and the heavy dots are the present model results. The Atwood number is A=0.5.

of the 2PF model introduced by Youngs [17] was presented by Freed et. al. [20]. In the self-similar 2PF solution [20], both f_i and u_i vary roughly linearly across the mixing zone, at all A. Thus, a good approximation for the effective diffusion coefficient is a parabolic shape:

$$D(x) = \begin{cases} \frac{1}{2}\frac{|U_1|+|U_2|}{|H_1|+|H_2|}[x - H_2][x + H_1] & H_2 < x < H_1 \\ 0 & \text{otherwise} \end{cases} \tag{11}$$

At the limit of low Atwood numbers, one can analytically show that D from the 2PF solution goes exactly to Eq 11. The effective diffusion coefficient from the 2PF solution is compared with Eq. 11 in Fig. 1 for $A = 0.5$. The agreement is seen to be good, and similar agreement is found for all A. In Fig. 2 the present model is compared with the 2PF model solution [20] and full-scale numerical simulation results in the self-similar regime. The numerical simulations started from an initial random multimode perturbation. The simulations were performed using Leeor-2D, a compressible, ALE

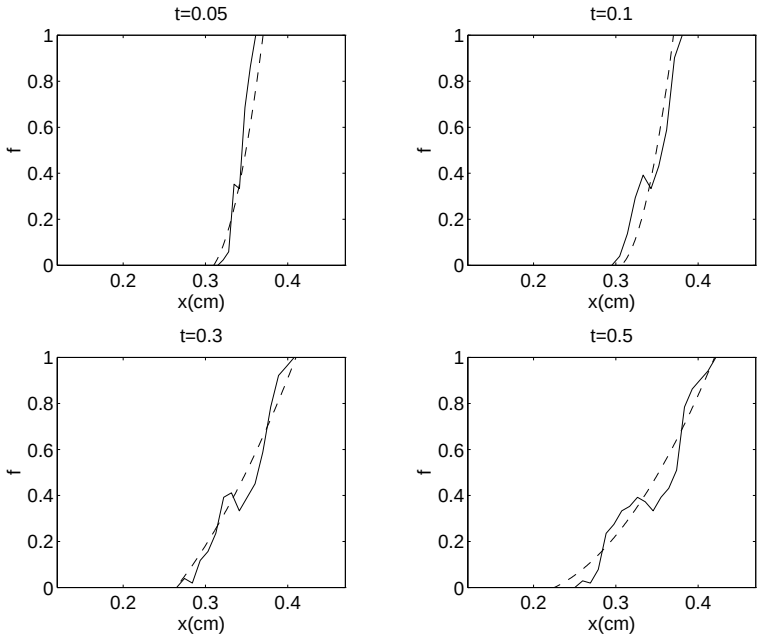

Figure 3: Heavy fluid volume fraction in a RM case. The full line is the simulation results, and the dashed line is the mixing model results, at various times, $t = 0.05, 0.1, 0.3, 0.5$ ms, representing both the early and late stages of the flow. The Atwood number is $A = 0.5$.

code with interface tracking [20]. The agreement between model and simulation is seen to be good.

We now turn to the RM case. We performed simulations with $g = 0$ and an initial multimode velocity perturbation [27]. In this case, there is no natural scale for the problem, such as the scale gt^2 in the RT case. In Fig 3, the volume fraction contours from the simulation and the model are compared at several times, both in the early and late stages of the flow (when the late-stage scaling laws already apply), at $A = 0.5$. The agreement is seen to be good. Similar agreement was found for all values of A [34].

4 Conclusions

A new realization of the 2PF approach was presented and applied for the RT and RM instabilities. The model simplifies standard 2PF treatments, separating the front evolution and the inner-zone mixing. The method advantages are easy and physically meaningful calibration of the front penetration based on large-structure physics, and a

numerically simple diffusion form for the inner zone mixing. The model was compared to 2D numerical simulations for classical, incompressible cases at various density ratios. Both RT and RM early and late-time growth and mixing profiles are well described with a single set of parameters. These parameters have been systematically derived by comparison with theoretical models. The mixing-model may be simply included in existing 1D hydrodynamic codes [36].

The present model should be viewed only as a first step towards an effective mixing model that includes the full physical effects in realistic problems. More complicated effects that require further study include the effects of compressibility, including loss of scale invariance in compressible RT problems [6], multiple shock passage [11, 12, 15, 21] and treatment of molecular level mixing [21, 27].

References

[1] D. Sharp, Physica D 12,3 (1984).

[2] R.D. Richtmyer, Commun. Pure Appl. Math. 13,297 (1960); E.E. Meshkov, Fluid. Dyn. ,101 (1969).

[3] S.W. Haan, Phys. Rev A 39,5812 (1989).

[4] D. Layzer, Astrophys. J. 122,1 (1955).

[5] C.L. Gardner, J. Glimm, O. McBryan, R. Menikoff, D.H. Sharp, Q. Zhang, Phys. Fluids 31,447 (1988); J. Glimm, X.R. Li, R. Menikoff, D.H. Sharp, Q. Zhang, Phys. Fluids A 2,2046 (1990).

[6] J. Glimm, D.H. Sharp, Phys. Rev. Lett. 64,2137 (1990); J. Glimm, Q. Zhang, D.H. Sharp, Phys. Fluids A 3,1333 (1991).

[7] U. Alon, D. Shvarts, D. Mukamel, Phys. Rev. E 48,1008 (1993).

[8] U. Alon, J. Hecht, D. Mukamel, D. Shvarts, Phys. Rev. Lett. 72,2867 (1994).

[9] U. Alon, J. Hecht, D. Ofer, D. Shvarts, Phys. Rev. Lett., 74,534 (1995).

[10] V.A. Andronov, S.M. Bakhrakh, E.E. Meshkov, V.N. Mokhov, V.V. Nikiforov, A.V. Penitskii, A.I. Tolshmyakov, Sov. Phys. JETP 44,424 (1976).

[11] C. E. Leith, "Development of a Two-Equation Turbulent Mix Model", UCRL-96036 (1986).

[12] S. Gauthier, M. Bonnet, Phys Fluids A 2,1685 (1990).

[13] V.A. Andronov, S.M. Bakhrakh, E.E. Meshkov, V.V. Nikiforov, A.V. Penitskii, A.I. Tolshmyakov, Sov. Phys. Doklady 27,393 (1982)

[14] D.C. Besnard, J.F. Haas, R.M. Rauenzahn, Physica D 37,227 (1989).

[15] D.C. Besnard, M. Bonnefille, P.B. Spitz, F.H. Harlow, R.M. Rauenzahn, "Turbulence Transport Modeling of Unsteady Multi-material Flows: Calibration of Model Constants", in Proceedings of the Third International Workshop on Physics of Compressible Turbulent Mixing, edited by R. Dautrey (DAM, Abbey of Royaumont, France, 1991).

[16] D.L. Youngs, Physica D 12,32 (1984).

[17] K.I. Read, Physica D 12,45 (1984).

[18] Turbulent transport terms may be added to 2PF models (discussed below) to describe local microscopic mixing inside the mixed region, while the large scale features are described by 2PF physics.

[19] N. Freed, D. Ofer, D. Shvarts, S.A. Orszag, Phys. Fluids A 3,912 (1991).

[20] D.L. Youngs, Physica D 37,270 (1989).

[21] M.J. Andrews, D.B. Spalding Phys. Fluids A 2,922 (1990).

[22] D.C. Besnard, F.H. Harlow, Int. J. Multi-phase Flow 14,679 (1988).

[23] C.W. Cranfill, Los-Alamos National Laboratory Report, LA-UR-92-2482, 1992.

[24] W.P. Crowley, E. Burke, private communication.

[25] F. Harlow, A. Amsden, J. Comp. Phys. 18,440 (1975).

[26] D.L. Youngs, Laser and Particle Beams 12,275 (1995).

[27] U. Alon, D. Shvarts, "Two Phase Flow Model for the Rayleigh-Taylor and Richtmyer-Meshkov Instabilities", to be published.

[28] J.W. Grove, R.L. Holmes, D. Sharp, "Numerical investigation of Richtmyer-Meshkov instability using front tracking", LA-UR-94-2024.

[29] Y. Yang, Q. Zhang, D.H. Sharp, Phys. Fluids 6 1856 (1994).

[30] D. L. Youngs, "Experimental investigation of turbulent mixing by RTI" Advances in Compressible Turbulent Mixing, edited by W.P. Dannevick, A.C. Buckingham and C.E. Leith (Princeton 1992) p. 607, Conf-8810234.

[31] H. Takabe, A. Yamamoto, Phys. Rev. A 44,5412 (1991).

[32] J. Hecht, U. Alon, D. Shvarts, Phys. Fluids, 6,4019 (1994).

[33] D. Ofer, D. Shvarts, Z. Zinamon, S.A. Orszag, Phys Fluids B 4,3549 (1992).

[34] U. Alon, D. Shvarts, to be published.

[35] R. Epstein, J.A. Delettrez, C.P. Verdon, U. Alon, D. Shvarts, "Simulations in 1D of Fuel-Pusher Mixing in Laser Driven Implosions", paper 2E9, Bull. Am. Phys. Soc. 40,1669 (1995).

[36] M.J. Dunning, S.W. Haan, Phys. Plasmas 2,1669 (1995).

[37] D. Shvarts, U. Alon, D. Ofer, C.P. Verdon, R.L. McCrory, Phys. Plasmas 2,2465 (1995).